
Composite Coatings Based on Renewable Resources Synthesized by Advanced Laser Techniques

Anita-Ioana Visan, Carmen-Georgeta Ristoscu and
Ion N. Mihailescu

Additional information is available at the end of the chapter

<http://dx.doi.org/10.5772/65260>

Abstract

This chapter reviews the progress and perspectives of composite materials in the form of thin films based on renewable resources for biofabrication of a new generation of medical implants with antibacterial properties. The chapter starts with an overview of the types of renewable materials that were currently studied and of the unique properties which make them perfect candidates for numerous bio-related applications. A briefing of recent progresses in the field of advanced laser synthesis of composites from renewable and sustainable materials, as well as the relevant results in our researches is made. The discussion spans composite coatings based on renewable resources, [e.g., chitosan (CHT) and lignin (Lig)] as biomaterials intended for metallic implants. A particular attention is given to lignin synthesis in the form of thin films due to its ability to functionalize the medical implant surface while preserving the similar composition and the structural properties of the raw, renewable biomaterial. We focused on recent technological advancements (e.g., matrix-assisted pulsed laser evaporation (MAPLE) and Combinatorial-MAPLE) which have brought the spotlight onto renewable biomaterials, by detailing the relevant engineering data of processing. This chapter concludes that the extensions of advanced laser techniques are viable fabrication methods of a new generation of metallic implants.

Keywords: Renewable, Chitosan, Lignin, MAPLE, C-MAPLE

1. Introduction

In this section, we made a short overview regarding classification of biocomposites, emphasizing the motivation of using biomaterials derived from renewable resources and highlighting

the current challenges in natural-derived biomaterials and their biomedical-related applications. We present relevant data regarding the properties of natural-derived and renewable biomaterials.





Biocomposites/biofibers			
Natural biopolymers			
Animal-based fibers		Wood-based natural fibers	Nonwood natural fibers
Proteins, like wool, spider, and silkworm <i>silk fibroin</i> [2]	Polysaccharides, chitin/ <i>chitosan</i> , glucose [3]	Cellulose, hemicellulose, and <i>lignin</i> , like flax, jute, sisal, and kenaf [4]	Straw fibers, bast, leaf, seed/fruit, grass fibers [5]
			

Table 1. Classification of renewable biopolymers used for biocomposites fabrication.

Biocomposites are a combination of natural fibers (e.g., wood fibers: hard and soft wood) or nonwood fibers (e.g., rice straw, pineapple, sugar cane, jute, flax, banana, etc.) with polymer matrices from both of the renewable and nonrenewable resources [1]. **Table 1** includes a classification of biocomposite biomaterials based on renewable resources [2–5].

In recent years, researchers focused on environmentally friendly composite based on natural fibers [6]. Because of their advantages, recent developments in composite based on renewable resources lead to improved biomaterials biofabrication with enhanced support for global sustainability [7].

In particular case of medical applications, biocomposite based on renewable materials have ability to support cell adhesion, migration, proliferation and differentiation; therefore, they can induce extracellular matrix formation and promote tissue repair [8]. An overview of recent reviews, book chapters and articles published in the field of renewable biomaterials is given in **Table 2**.

Relevant data regarding the properties of natural renewable biomaterials with related results presented in this chapter are introduced.

Polysaccharide-based biopolymers are of considerable interest as a source of renewable materials with applications in the biomedical, food, textile and energy industries [22].

Between them, chitin derivatives are widely studied [e.g., chitosan (CHT)]. Since chitosan is biocompatible and biodegradable, an ample diversity of interesting studies based on chitosan were reported [22].

Chitosan has been explored as a scaffold for tissue engineering due to its significant osteoconductivity, but minimal osteoinductive property [23, 24]. Chitosan has been prepared in various geometries such as thin films, scaffolds, sponges, fibers or other complex structures, for biomedical applications [25, 26].

The chitosan incorporation in composite biomaterials enhances the mechanical property of the basic biomaterial. In Ref. [27], it was proved an increase in compressive strength by 33.07% and an enhancement of the proliferation of mouse preosteoblastic cells (MC3T3-E1) upon addition of nano-hydroxyapatite (nHA) to chitosan. Another example is given by Venkatesan et al. [28] which evidenced that the blending chitosan with an anionic polysaccharide alginate may stabilize the system by electrostatic interaction of them.

Renewable materials	Applications	References
Thermosetting materials, plant oils, polysaccharides, lignin, phenolics, epoxy, unsaturated polyester and polyurethane resins and proteins	Non-food applications	[9]
Polysaccharides and their derivatives, lignin, suberin, vegetable oils, tannins, natural monomers like terpenes, and monomers derived from sugars, with particular emphasis on furan derivatives and lactic acid, bacterial cellulose, and poly(hydroxyalkanoates)	Biomedical application Biomass	[10]
Vegetable oils, lignin, proteins, natural polysaccharides	Bioplastics; bioasphalt; biofuel; biomass; medical applications	[11]
Biocomposites natural fiber bioplastic cellulosic plastic polyactides poly(hydroxyalkanoates) soybean-based plastic fiber-matrix interface	Industrial ecology; green chemistry; agricultural and biomass feedstock	[12]
Plant oil-clay hybrid materials	Green nanocomposites	[13]
Ryegrass (<i>Lolium perenne</i> X <i>multiflorum</i>) and alfalfa (<i>Medicago sativa</i> subsp. <i>Sativa</i>)	Production of leaf protein concentrate; green biorefinery	[14]
Cellulose nanocrystals (CNC)	Biomedical application	[15]
Oil palm	Biofuel production	[16]
Lignin	Production of chemicals, materials, and fuels from renewable plant resources	[17]
Algae-derived hybrid polyester	Scaffolds for bone, cartilage, cardiac and nerve tissue regeneration	[18]
Polymers from biomass; polysaccharides; lignin; plant oils; terpenes and rosin; glycerol; sugars; furans	Bioplastics; bioasphalt; biofuel; biomass; medical applications	[19]
Chitosan; poly(vinyl butyral)	Anti-corrosion coatings	[20]
Polysaccharide-based biopolymers especially starch, cellulose, chitin, chitosan, alginate	Waste-water treatment; drug-delivery systems	[21]

Table 2. Overview of recent reviews, book chapters and articles published in the field of renewable biomaterials.

Other studies have been dedicated to chitosan and its biocomposite scaffolds investigations under *in-vivo* conditions. Ma et al. [29] demonstrated that chitosan/gelatin scaffolds degraded completely in 12 weeks, while promoted osteoblast proliferation *in-vivo*.

As well as chitosan, lignin (Lig) is a renewable and a natural polymer [30]. This complex, amorphous organic polymer consists in a natural matrix which binds the strong and stiff cellulose units together, generally in natural wood. Lignin has been studied due to its antioxidant and antimicrobial properties, making it the perfect candidate for biomedical applications [31].

In the study of X. Pan et al. [32], lignin prepared from hybrid poplar wood chips exhibited higher antioxidant activities based on 1,1-diphenyl-2-picrylhydrazyl (DPPH) assay. In the same time, in Ref. [33], it is reported that Kraft lignin from wood sources in pulp industry can protect the oxidation of corn oil, being as efficient as vitamin E.

Nada et al. [34] demonstrated the lignin antimicrobial activities toward some bacteria and fungi-like Gram-positive bacteria (*Bacillus subtilis* and *Bacillus mycoides*).

The lignin incorporation in composite biomaterials led to biofabrication of new compounds with enhanced bioactivity and osteoconductivity [35, 36]. An unaltered incorporation of lignin provides a composite with enhanced stability and improved interconnected structure, while increasing the coating cohesion, as showed in Refs [37, 38].

Renewable resources have therefore a functional role in providing easily available and often cheap biomaterials for biofabrication of new generation of implants.

2. Laser-assisted strategies for renewable resources with medical applications

In this section, we present the current strategy in laser-assisted synthesis (emphasizing the challenges and limitations) and the potential biomedical applications of deposited/obtained coatings. An up-to-date example of composites based on natural biopolymers for medical applications by means of laser-assisted processing is given.

The development of bionanotechnology based on laser techniques holds out great promise of improvements in the quality of life, including new treatments for disease providing a high potential for the fabrication of antimicrobial coatings for orthopedic implants [39].

Several techniques for the synthesis of thin films based on renewable resources such as spin-coating [40], dip-coating [41], spray-coating [42], as well as laser methods, such as laser-induced forward transfer [43], matrix-assisted pulsed laser evaporation (MAPLE) [44], Combinatorial-MAPLE [45]; resonant infrared (RIR) MAPLE [46] and MAPLE direct write [47] are currently used.

In spite of the vast list reported in the literature of biomaterials deposited in form of thin films, each of the above-mentioned methods have some limitations in terms of coating thickness, multilayer deposition, adherence, composition or crystallinity. **Table 3** summarizes the generally used biomaterials based on renewable resources and deposition methods along with specific advantages and drawbacks.

Biomaterials and performance/application	Deposition method	Advantages	Disadvantages
Lignin extracted from sugar cane bagasse [48]	Physical vapor deposition (PVD)	High temperature and good impact strength, excellent abrasion resistance, improved corrosion resistance	Line-of-sight transfer, operate at very high temperatures and vacuums, requires a cooling water system to dissipate large heat loads
Silver/hydroxyapatite/lignin [49]	Electrophoretic deposition (EPD)	Lower costs, simpler and less complex control requirements; application to both organic and inorganic coatings	Poor coating adhesion
Nano-TiO ₂ /silk fibroin [50]	Sol-gel (SG)	Macroporous bioactive scaffold	Poor coating adhesion; involvement of liquid media limit multi-layer assembling (affect interfaces)
Lignin [51]	Spin coating	Simple, uniform coatings	Solvent issue during multilayers, adherence
Acacia lignin-gelatin [52]	Casting	Monolayers	Limited to very thin films
Simple and silver-doped hydroxyapatite lignin [53]	Matrix assisted pulsed laser evaporation (MAPLE)	Application to both organic and inorganic coatings, multilayers and multistuctures	Small covering areas
Fibronectin (FN) and poly-dl-lactide (PDLLA) [45]	Combinatorial matrix-assisted pulsed laser evaporation (C-MAPLE)	Simple, single step, fabrication route which can easily limit the time of manipulation and biomaterials consumption	Composition gradient is hard to discriminate in case of compounds with similar chemical structures

Table 3. Biomaterials from renewable resources, deposition methods, advantages and drawbacks.

Between all techniques, laser-based technologies are exhibiting a lot of advantages, as: fabrication of a wide range of different biomaterials, controlled film thickness, good adhesion to substrate [55]. Furthermore, laser-based technologies imply a low material consumption and ensure the stoichiometry preservation of the growing films [39].

Next, relevant data regarding the laser processing techniques used for fabrication of medical implants based on renewable materials are presented. Concretely, the discussion spans the MAPLE and C-MAPLE techniques.

MAPLE technique proved to be a safe approach for transporting and depositing delicate, heat sensitive molecules. Recent comprehensive reviews on MAPLE deposition of organic, biological and nanoparticle thin films exemplified a large potential in medicine, biology, pharmaceuticals or drug delivery applications of thin coatings obtained by this method [56].

The MAPLE experimental setup is presented in **Figure 1**.

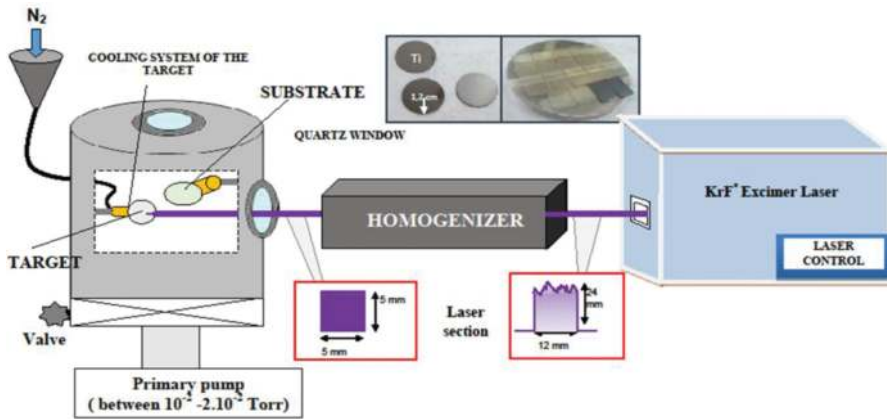


Figure 1. MAPLE experimental setup.

MAPLE target consists of starting material (<10 wt.%) dissolved or suspended into a laser wavelength absorbing solvent when in frozen state. The biomaterial molecules achieve enough kinetic energy by collective collisions with the evaporating solvent molecules, guarantying a controlled transfer on the substrate while being efficiently pumped away by the vacuum system.

By most favorably adjusting the MAPLE deposition parameters (e.g., laser wavelength, laser fluence, repetition rate, solvent type, solute concentration, substrate temperature, background gas nature and pressure), the process can be performed without considerable biomaterial decomposition [38, 57].

Concomitantly, remarkable efforts were recently focused on the development of combinatorial processes for biofabrication of new biomaterials with innovative properties. Typically, the fabrication of a composite layer is carried out by premixing of biopolymer solutions followed by heating of coating [58] or film casting/solvent evaporation [59]. The combinatorial technology for the blending of two different biomaterials [45, 60–62] is based on MAPLE process (Figure 2).

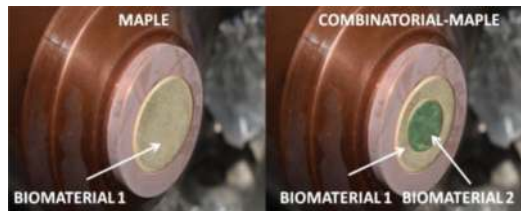


Figure 2. Target holder in the case of MAPLE (left) and combinatorial-MAPLE (right) techniques.

This brand new developed technique—Combinatorial-MAPLE—stands for a simple, single step, biofabrication path which can easily limit the time of manipulation and biomaterials consumption [55].

In C-MAPLE experiments, the two targets (e.g., Biomaterial 1 and Biomaterial 2) were concurrently evaporated by the laser beam, which was divided into two beams (Figure 3) by an optical splitter. The two beams were focused in parallel onto the surface of each target, containing the frozen solutions to be irradiated. A gradient of composition from 100% Biomaterial 1 to 100% Biomaterial 2 is thus obtained on a substrate, as schematically represented in Figure 4.

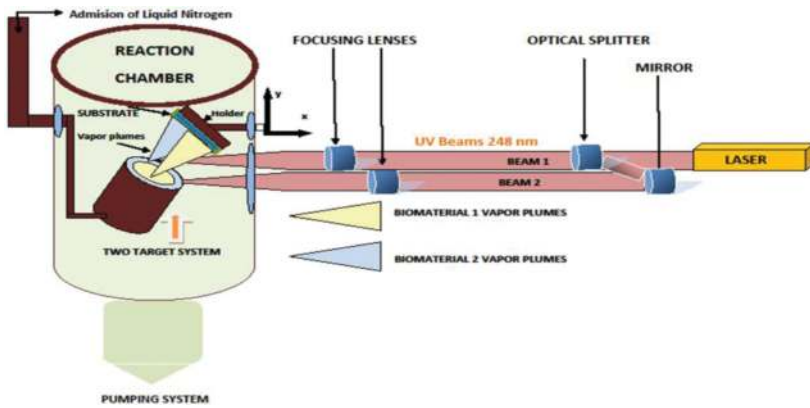


Figure 3. Combinatorial-MAPLE experimental setup.

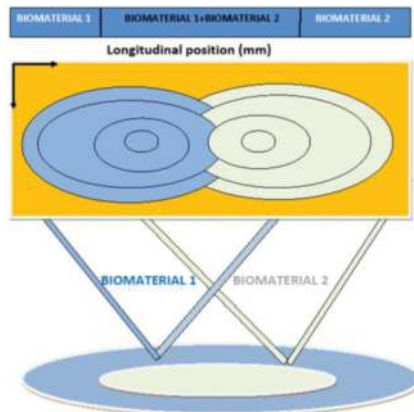


Figure 4. Schematic representation of the thin film gradient structure growth and components intermixing developed by C-MAPLE.

C-MAPLE technique offers the possibility to combine and immobilize two or more biomaterials, dissolved in different solvents, using diverse wavelengths. Next, by physical, chemical and biological characterization of the obtained structures, one may select the best compositions that can be synthesized from the two biomaterials.

MAPLE and C-MAPLE techniques could unlock the research frontiers in biofabrication of composite based on renewable resources with great potential for various applications.

3. Relevant results regarding renewable materials deposited by advanced laser techniques: trends and challenges

In this section, relevant data regarding the engineering of novel renewable materials by laser processing and their applications are detailed.

3.1. The literature survey of renewable materials-based composites deposited by laser techniques

In this chapter, we focused biomaterials based on renewable resources in form of thin films fabricated by laser-based concepts for obtaining functionalized medical implants. The first example refers to silk fibroin and composite HA-fibroin coatings deposited by MAPLE [63]. Silks are fibrous proteins synthesized in specialized epithelial cells of Lepidoptera larvae such as silkworms, spiders, scorpions, flies and mites.

The studies of Miroiu et al. [63] showed that compared to the simple fibroin or HA thin films, obtained implants exhibit an intermediary topography, favorable to bone cells anchorage and proliferation. On the same time, it resulted that the fibroin content in films was a mixture of preponderantly random coil with crystalline forms, β -sheet and α -helix. The renewable silk fibroin composite evidenced by *in-vitro* viability tests appropriate bone cell behavior nontoxicity, good spreading and normal cell morphology [63].

Next, biocomposite silk fibroin-poly(3-hydroxybutyric-acid-co-3-hydroxyvaleric-acid) biodegradable functionalized implants were grown by MAPLE [64]. Silk fibroin and poly(3-hydroxybutyric-acid-co-3-hydroxyvaleric-acid—PHVB) are both natural biopolymers with excellent biocompatibility, but different biodegradability rates and tensile strength properties. They were combined in a composite in order to improve their properties as coatings for biomedical uses. The physical-chemical properties of the composite coatings and principally their degradation behavior in simulated body fluid were investigated as primary step of applicability in local controlled drug release. It was demonstrated that higher PHVB contents enhance the resistance and lead to a slower degradation rate of composite coatings [64].

Another MAPLE studies related to synthesis of poly(D,L-lactide-co-glycolide) (PLGA) particle systems were reported by Socol et al. [65]. PLGA + polyvinyl alcohol (PVA), PLGA + PVA + bovine serum albumin (BSA) and PLGA + PVA + chitosan nanoparticles were prepared by an

oil-in-water emulsion-diffusion-evaporation method and afterwards were transferred in form of thin film for local-controlled drug delivery. *In vitro* investigations exhibited that the distribution and morphology of osteoblast-like SaOs-2 cells on some PLGA particle coatings were comparable with that of control [65].

Further, considerable attention has been focused on development and utilization of secondary metabolites of plants (phytochemicals) as a substitute to and/or in combination with traditional antibiotics for treating infections. Between the phytochemicals, flavonoids are perfect candidates because they are extensively distributed in edible plants and possess broad pharmacologic activity [66]. Flavonoids are a group of heterocyclic organic compounds frequently found in vegetables, fruit, flowers, nuts, wine, seeds, stems, tea, honey and propolis [66]. Composite thin films of biopolymer (polyvinylpyrrolidone), flavonoid (quercetin dihydrate and resveratrol)-biopolymer and silver nanoparticles biopolymer were deposited using MAPLE method demonstrating the anti-inflammatory, antispasmodic, anti-allergic and antimicrobial properties obtained effects [66].

Furthermore, C-MAPLE was used for transfer and immobilization of Fibronectin (FN) and poly-D,L-lactide as a new strategy for the controlled release applications of biologically active substances as proteins and drugs [45].

3.2. Case study: lignin-based biocomposites

This subsection is intended to summarize the recent progresses and concerns involving the use of lignin in the development of new polymer biocomposite materials for high performance medical implants applications.

Until now, biocomposite coatings based on the renewable lignin were studied by electrophoretic deposition (EPD) only [36, 37], and the results revealed that the obtained composite exhibited enhanced stability and improved interconnected structure, with an increased coating cohesion [53]. For electrophoretic deposition (EPD) method, it was applied a constant voltage (at optimized parameters 60 V for 45 s), and it were obtained uniform composite coatings with good adhesion and mechanical properties without any phase transformation [67].

In our studies, we report MAPLE deposited a large macromolecule of undefined molecular weight-organosolv lignin (Lig) embedded in a simple hydroxyapatite (HA) or silver (Ag) doped hydroxyapatite film matrix [53]. A pulsed KrF* laser source ($\lambda = 248 \text{ nm}$, $\zeta_{\text{FWHM}} = 25 \text{ ns}$) operating at 10 Hz was used for the Ag/HA/Lig and its counterpart without silver (HA/Lig) composite frozen targets evaporation. Pure titanium foils or silicon wafers were used as substrates. A total number of 20,000 pulses at a fluence of 0.7 Jcm^{-2} were applied for the deposition of each structure while the spot size was of 25 mm^2 . Then, the structures were subjected to analysis by scanning electron microscopy (SEM), energy-dispersive X-ray spectroscopy (EDS), X-ray diffraction analysis (XRD), X-ray photoelectron spectroscopy (XPS) and attenuated total reflectance-Fourier transform infrared (ATR-FTIR) [53].

Smooth, uniform Lig-based thin films adherent to substrate were revealed by typical top-view SEM images (Figure 5). As a first observation, rough surface of the films was reported starting

from the same nano-hydroxyapatite powder composite with Lig, when using the electrophoretic deposition [67] (**Figure 6**).

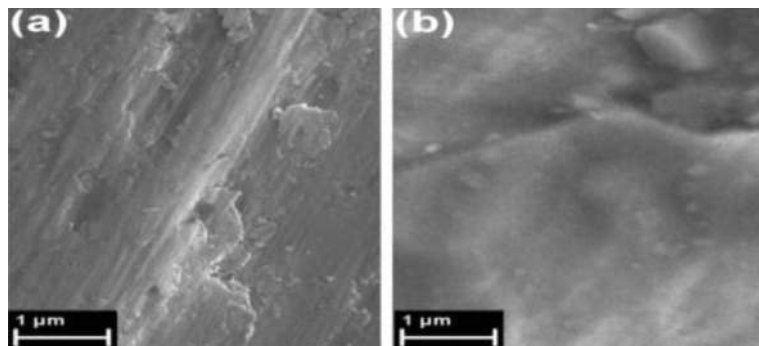


Figure 5. Top-view SEM micrographs of the HA-Lig (a) and Ag:HA-Lig films (b) deposited by MAPLE on Ti substrates. Reproduced with permission from Ref. [53].

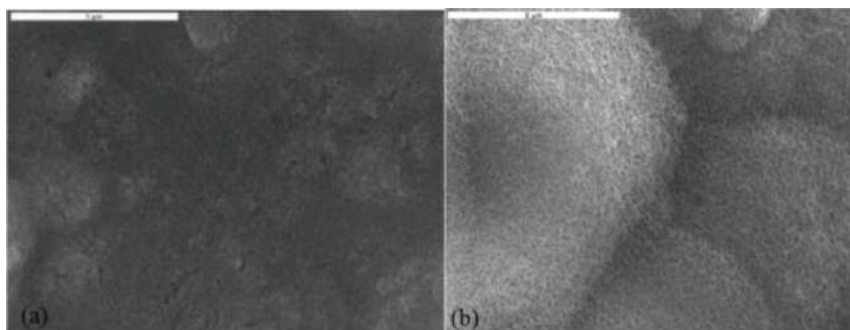


Figure 6. SEM micrographs of sintered Ag/HAP/Lig coating (a) before and (b) after immersion in SBF solution at 37°C. Scale bar: 5 μm. Reprinted from Ref. [67] with permission. Copyright American Chemical Society 2013.

EDS analyses revealed the presence of HA components but also evidences of traces of Ag and lignin. The deposited HA was Ca deficient, which denotes a film with increased solubility. Recorded X-ray patterns (data not presented) were characteristic to amorphous films. Lignin presence in composite films was undoubtedly proved by both XPS and FTIR. The XPS spectra were achieved for two films: the composite Ag:HA-Lig and the pure HA film one (**Figure 7**). The lignin dispersion in HA matrix was evidenced by the massive increase in the C-bonded carbon signature, accompanied by a slight raise of the constituent connected with oxygen-bonded C or oxygen-containing radicals. These enhancements were attributed to the lignin presence. The certain proof that lignin has been successfully transferred into the HA composite film consist in calculated experimental data regarding the stoichiometry fraction $x\text{C}:y\text{O}$ considering the addition of 10% lignin into the HA matrix.

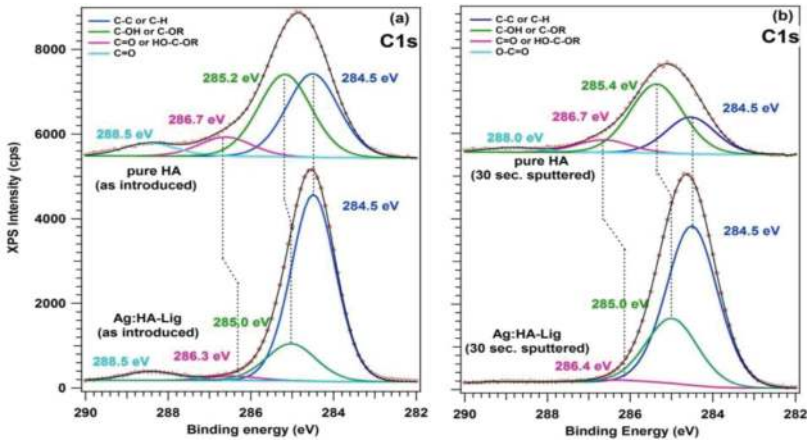


Figure 7. C 1s core level high resolution XPS spectra for the pure HA (a) and Ag:HA-Lig (b) MAPLE films. Reproduced with permission from Ref. [53].

HAP/Lig, wt.% Lig	Thermal treatment	Ca	P	C	Ca/P
HAP	Non-sintered	19.4	11.3	7.2	1.72
	Sintered	16.5	5.5	21.7	3.00
0.5	Non-sintered	19.1	11.3	8.2	1.69
	Sintered	18.4	7.9	15.9	2.33
1	Non-sintered	19.3	10.8	10.5	1.79
	Sintered	18.7	8.9	11.3	2.10
3	Non-sintered	18.4	12.0	11.7	1.53

Adapted from Ref. [67] with permission. Copyright Elsevier 2016.

Table 4. Quantitative XPS analysis data for Synthetic hydroxyapatite, $\text{Ca}_{10}(\text{PO}_4)_6(\text{OH})_2$ (HAP) and hydroxyapatite/lignin (HAP/Lig) (0.5–10) wt.% Lig electrophoretic coatings.

According to the Ref. [67], in the electrophoretic deposition case, lignin limited the decomposition of the apatite lattice of sintered composite coatings based on Lig with (1–10) wt.% Lig. This was designated by the smaller increase in carbon content and decreased Ca/P ratio, compared to pure apatite coating and HAP/Lig coating with 0.5 wt.% Lig (Table 4).

In addition, FTIR investigations advocated a certain improvement of Lig-based films mechanical properties due to lignin incorporation (Figure 8). In good agreement with FTIR observations in the case of MAPLE method, it is also noticed for electrophoretic deposition that does not occur with any alteration of the initial material. This fact could be associated with the binding of hydroxyls from apatite lattice, preventing the decomposition and/or ion diffusion on substrate surface, demonstrating that Lig protects HAP/Lig coatings [68].

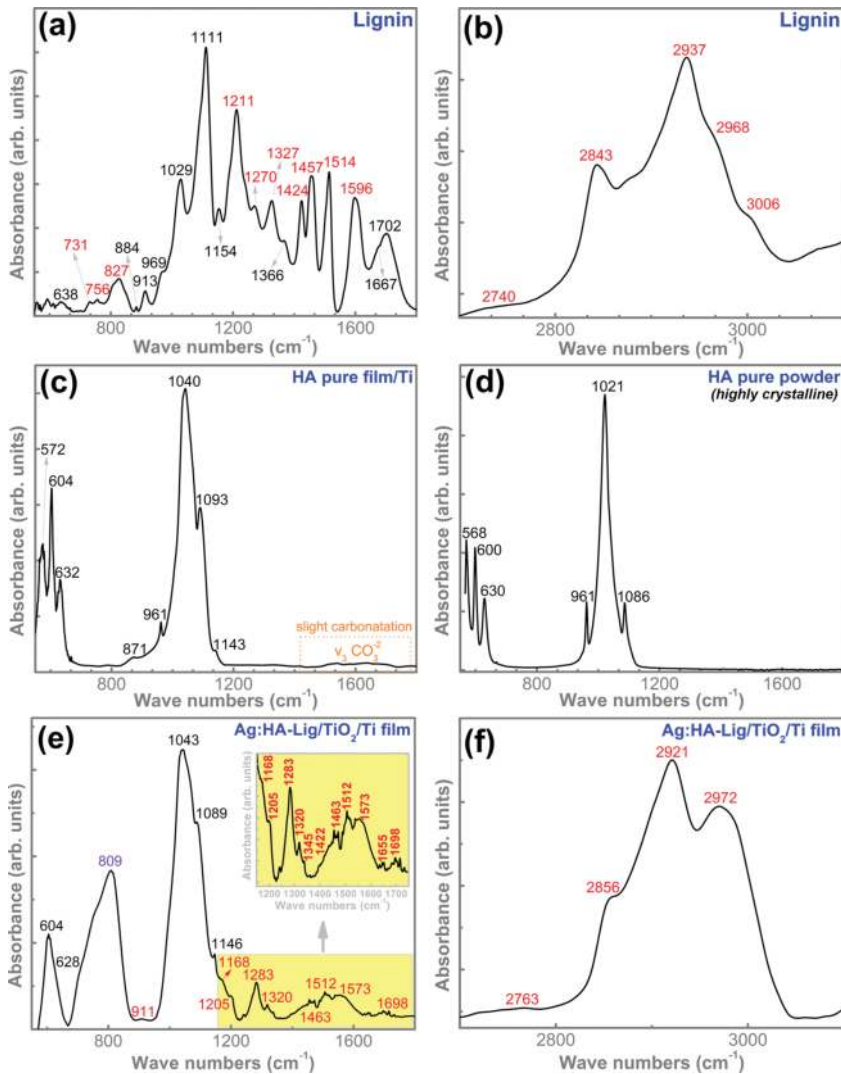


Figure 8. ATR-FTIR spectra of Lig powder (a,b), pure HA film (c), pure HA powder (Sigma-Aldrich) (d) and Ag:HA-Lig film (e,f) in the spectral regions: 1800 – 550 cm^{-1} (a,c,d,e) and 3100 – 2700 cm^{-1} (b,f). Reproduced with permission from Ref. [53].

The validation of the MAPLE technique was demonstrated for deposition of such delicate renewable biomaterial, as suggested by EDS, XPS, FTIR, biological and microbial results. The MAPLE obtained biocomposites-based Lig were found noncytotoxic, promoting the proliferation of the adhered human mesenchymal cells (figure not shown here) [53], while the microbiological assays revealed that the coated composite assured a prolonged release of silver

ions, exhibiting a high both bacterial and fungal behavior (**Figure 9**). The same comportament was noticed in the case of the other reported electrophoretic case (**Table 5**) [68], where lignin addition both boosted the antimicrobial activity and supported the normal development and growth of the adhered cells [68].

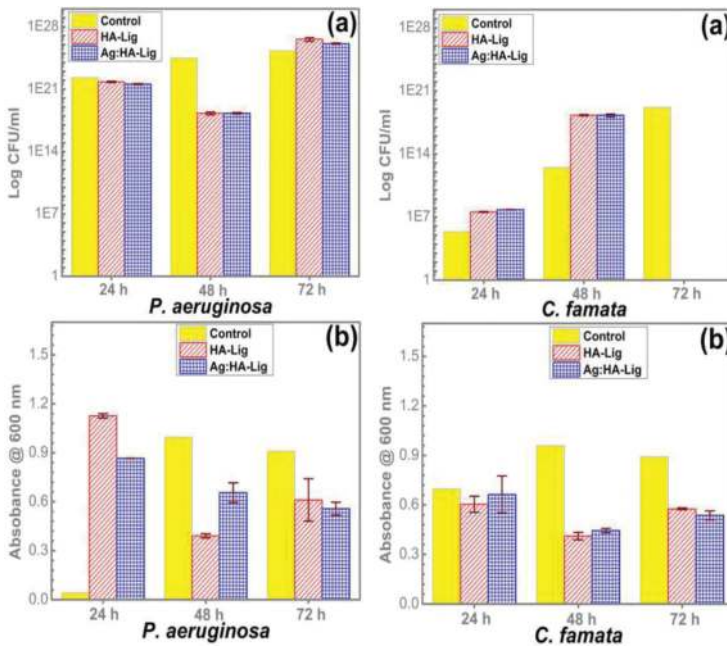


Figure 9. (a) Number of *Pseudomonas aeruginosa* and *C. famata* viable cells recovered from the biofilms growing on the tested specimens after 24, 48 and 72 h, respectively (b) Absorbance values at 600 nm of the *P. aeruginosa* and *C. famata* bacterial biofilm developed on the tested specimens after 24, 48 and 72 h, respectively. Adapted with permission from Ref. [53].

Bacteria strain type	<i>Staphylococcus aureus</i> TL		
Initial	1 h	24 h	
Control (CFU mL ⁻¹)	1.0 × 10 ⁵	3.0 × 10 ⁴	9.9 × 10 ⁴
Ag/HAP/Lig (CFU mL ⁻¹)	2.5 × 10 ⁴	2.0 × 10 ³	No bacteria

Reprinted from Ref. [68] with permission. Copyright Elsevier 2016.

Table 5. Reduction of viable cell number of *Staphylococcus aureus* TL after incubation with Ag/HAP/Lig coating for 0, 1 and 24 h.

Biofabrication of composites based on Lig-renewable resources have a great potential for medical applications, supporting the osteogenic cell proliferation while assuring an antibacterial behavior.

3.3. Case study: chitosan-based biocomposites

This subsection is intended to summarize the recent progresses and concerns involving the use of chitosan in the development of new biocomposite materials for high performance medical implants applications.

Although many authors have reported the preparation of mixtures of chitosan and calcium phosphates in the form of powders [69], membranes [70], scaffolds [71] or microspheres [72], only few publications were dedicated on developing new procedures allowing the concomitant preparation of a biocomposite material containing the two components, which is predicted to assure a more close contact between them [73–75]. For this reason, further we will exemplify the biofabrication of the compositional map of chitosan (CHT) and biomimetic apatite (BmAp) by the innovative C-MAPLE technique. In the experiments, an excimer laser source (KrF^* , $\lambda = 248 \text{ nm}$, $\zeta_{\text{FWHM}} = 25 \text{ ns}$) operated at 10 Hz frequency repetition rate was used for the cryogenic targets evaporation. As deposition substrates were used as follows: 12 mm diameter Ti (grade 4) disks, Si wafers or glass slides. The coated samples areas deposited onto the substrate selection formed of five consecutive 12 mm Ti disks which are further denoted S1–S5; where S1 stands for the coating area having CHT as major component, S5 represents the coating area with richer content of BmAp. S2–S3–S4 series indicates blended coating areas with decreasing CHT/BmAp ratios. For comparison reasons, simple CHT and BmAp films have been also deposited on the same type of substrates [54]. After preliminary studies, deionized water was chosen as solvent to prepare solutions of 1 and 2 wt.% for CHT and BmAp, respectively. A parametric study in order to find the optimum laser energy (70, 100, 120 and 150 mJ) for which the materials are deposited unaltered was performed. The selected laser energy was as follows: 100 mJ in the case of CHT target and of 70 mJ for the BmAp one.

C-MAPLE composite coatings have a homogeneous spongy appearance all over the substrate, which is known to be beneficial for cell adhesion as revealed by SEM micrographs (results not presented here). While CHT particulates preserve their spherical morphology, elongated filiform structures can be also noticed in the blended regions of the film (S2–S4). One can assume that these thread-like structures may support some toughness improvements similar to the one provided by fiber reinforcing in the biocomposite materials, ensuring the desired mechanical behavior for tissue substitution [76].

The C-MAPLE synthesized biocomposite-based CHT thin films are amorphous, rough, with a morphology characteristic to laser deposited structures. Next, by high resolution AFM investigations, we disclose information about the nanostructuring of the film grains and their morphological evolution (**Figure 10**). One notices that a progressive increase in roughness (R_{RMS}) occurs with the CHT concentration in the C-MAPLE composite films [54].

For each combinatorial surface, the Ca/P molar ratio was in the range ~ 1.3 – 1.5 , lower than the stoichiometric theoretical value of hydroxyapatite (i.e., 1.67), pointing to the calcium-deficient state of biomimetic apatite synthesized.

The Raman spectra of BmAp, HA (pure and highly crystalline) and CHT raw materials are presented comparatively in **Figure 11a** and **b** [54]. Similar vibration bands to the ones revealed by FTIR investigations (data not shown here) [54] have been also identified by micro-Raman

analyses for the CHT and BmAp source materials. However, in the case of Raman spectra the symmetric stretching bands are now the dominant ones (e.g., symmetric stretching ν_1 of $(\text{PO}_4)^{3-}$ $\sim 956 \text{ cm}^{-1}$; symmetric stretching of aliphatic (C–H) bonds $\sim 2929 \text{ cm}^{-1}$). This is owed to the fact that in Raman spectroscopy, the vibration bands intensity is dependent on the polarizability induced dipole, and not on the variation of the dipole moment of the molecule, as is the case of FTIR spectroscopy. Thereby, this was to be expected, as for a given centrosymmetric molecule, the vibration modes which are symmetric to the inversion center of the molecule generate higher Raman intensity bands. Moreover, the electronic density between the carbon atoms in aliphatic C–H bonds that can be deformed under the action of the radiation electric field should be large. If the vibrational mode involved in the Raman scattering process is not totally symmetric, then the polarization of the photon can be partially (e.g., antisymmetric stretching modes) or even totally reduced.

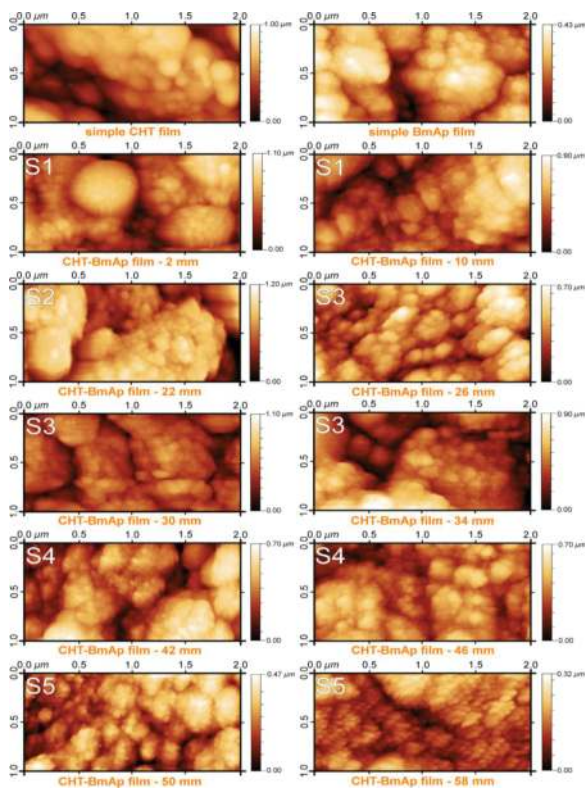


Figure 10. Comparative AFM images recorded on the surface of: simple CHT and BmAp films deposited by MAPLE, and in various regions of the C-MAPLE composite film starting from the CHT-rich edge. The coated samples areas deposited onto the substrate array composed of five consecutive 12 mm Ti disks were denoted S1 to S5; where S1 stands for the coating area having CHT as major component, S5 represents the coating area with richer content of BmAp. S2-S3-S4 series indicates blended coating areas with decreasing CHT/BmAp ratios.

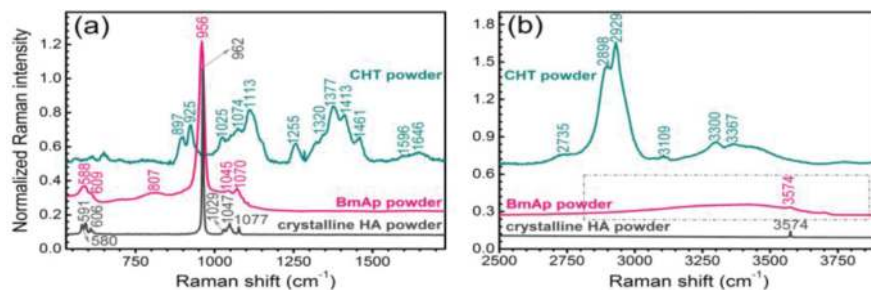


Figure 11. Comparative Raman spectra of BmAp, crystalline HA and CHT powders presented in the fingerprint (a) and functional groups (b) regions. The spectra have been normalized to the highest intensity peak (i.e., $\nu_1(\text{PO}_4)^{3-}$ vs. C-H bands in the case hydroxyapatite and chitosan, respectively).

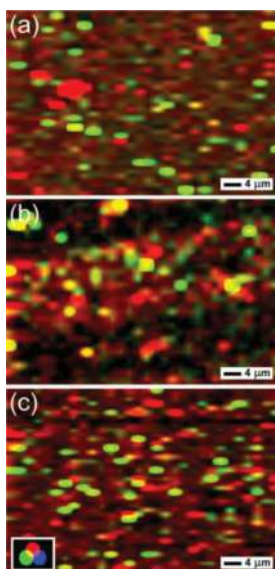


Figure 12. 2D Raman maps obtained from $(80 \times 100) \mu\text{m}^2$ areas of the CHT-BmAp composite C-MAPLE film, based on the characteristic Raman stretching vibration bands of C-H bond in aliphatic and aromatic groups ($3000\text{--}2850 \text{ cm}^{-1}$ wave numbers region) of CHT (red colored), and ν_1 symmetric stretching of orthophosphate groups ($965\text{--}950 \text{ cm}^{-1}$ wave numbers region) of BmAp (green colored). (a) CHT-rich edge region (b) CHT-BmAp central region (c) BmAp-rich edge region.

In perfect agreement with the FTIR results, the Raman spectra indicated that the BmAp material elicit a decreased ordering (indicated by the broader aspect of the bands) and a certain level hydration with respect to the pure and crystalline HA.

The CHT vibration bands in the $1250\text{--}1000 \text{ cm}^{-1}$ wave numbers region are screened by the more intense superimposed Si-O-Si stretching band of the glass substrate (**Figure 12**). Overall, the

CHT and BmAp bands in the case of the composite C-MAPLE films are less conspicuous and defined with respect to the ones of the source powders. The shift of ν_1 symmetric stretching band of $(\text{PO}_4)^{3-}$ groups close to $\sim 956 \text{ cm}^{-1}$ with respect to the stoichiometric crystalline compound (i.e., $\sim 962\text{--}961 \text{ cm}^{-1}$) suggest a higher degree of disordering, similarly to the source BmAp material.

Subsequently, X-Y Raman mapping measurements have been performed in three relevant regions (with areas of $(80 \times 100) \mu\text{m}^2$) of the C-MAPLE synthesized biocomposite-based CHT thin films deposited onto glass substrate (**Figure 12**), in order to generate detailed chemical images (in red-green-blue colors) of the spatial distribution of the two species (i.e., CHT and BmAp). The CHT phase (red colored) has been integrated with the stretching vibration bands of C–H bond in aliphatic and aromatic groups ($3000\text{--}2850 \text{ cm}^{-1}$ wave numbers region), while the BmAp phase (green colored) has been assigned with the prominent Raman band of HA (i.e., $\nu_1(\text{PO}_4)^{3-}$ symmetric stretching) situated in the $965\text{--}950 \text{ cm}^{-1}$ range. The distribution of CHT seems to be homogenous in all analyzed composite film regions, whilst the BmAp phase is rather distributed in randomly dispersed aggregates.

XPS analysis confirmed the chemical composition of the C-MAPLE synthesized biocomposite-based CHT thin films. XPS survey spectra collected on the surface of CHT-BmAp samples (not presented) indicated the presence of C 1s, O 1s, N 1s, Ca 2s, Ca 2p, P 2s and P 2p photoelectron peaks [54], while **Figure 13** showed the atomic ratio $\text{N } 1s/(\text{N } 1s + \text{Ca } 2p)$ evolution depending on the position of material deposited along the CHT-BmAp blended sample. As predicted, the atomic ratio ($\text{N } 1s/\text{N } 1s + \text{Ca } 2p$) is decreasing from CHT to BmAp compounds, evidencing the composition gradient of the combinatorial films.

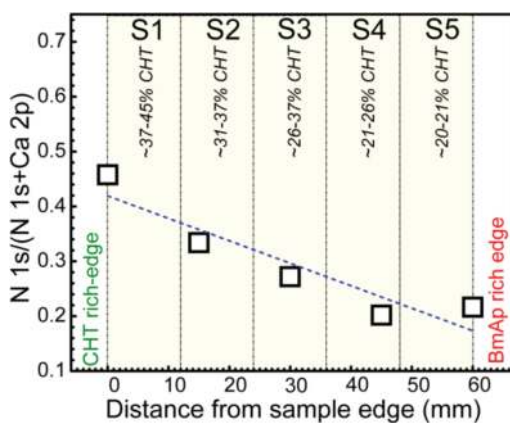


Figure 13. Typical XPS measurement along the composite CHT-BmAp C-MAPLE films. Reproduced with permission from Ref. [54].

The antimicrobial activity was controlled by the concentration of chitosan, the most efficient antimicrobial activity, against Gram-positive and Gram-negative strains, was assigned to blended S3 and S4 samples (**Figure 14**).

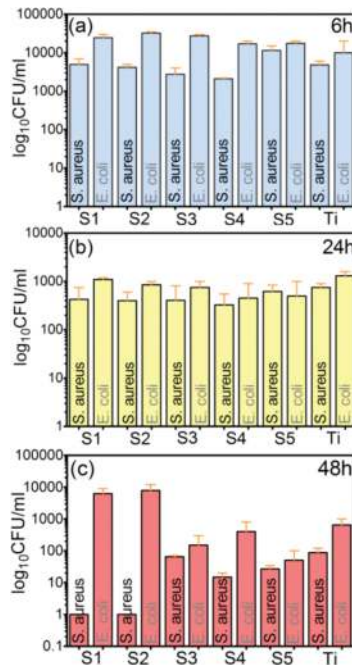


Figure 14. Graphic representation of the number of viable microbial cells adhered to the surface of CHT-BmAp composite film after (a) 6 h (b) 24 h and (c) 48 h of incubation. Reproduced with permission from Ref. [54].

The composition gradient of the chitosan-to-biomimetic hydroxyapatite has been confirmed longwise the combinatorial films by FTIR and XPS analyses, validating the used C-MAPLE technique.

C-MAPLE technique used in this study proves to be a prospective and viable method for the fabrication of biomimetic and bioactive antimicrobial orthopedic coatings based on renewable resources which resemble the native bone extracellular matrix while creating a favorable living environment for osteogenic cells, in the same time assuring protection from microbial colonization.

4. Conclusions and future perspectives

This chapter is intended to provide a brief outline of work that covers biocomposites based on renewable resources which have been studied and applied in medical applications, capable of supporting cell proliferation and biodegradability.

The raw substances used for depositions are renewable and the whole procedure is very accurate due to the cumulative advantages of substances origin and applied laser procedures. A credible demonstration for the conservation of biomaterial composition, structure, mor-

phology and the most probably functionality was made of the MAPLE and C-MAPLE transferred films.

In this way, multifunctional structures could be deposited with combined bioactive osteoinductive and/or antimicrobial action. The synthesized multistructures were considered for use as biomimetic coatings of advanced implants but also as a shield against infections including microbial biofilms. This feature can play a key role in the development of a new generation of drug delivery systems based on renewable resources free of infection with microbial biofilms which cannot be annihilated with the existing generation of antibiotics.

Acknowledgements

The authors acknowledge the financial support of UEFISCDI under the France-Romania bilateral contract: 778/2014, 19_RO-Fr/2014, PCCA 244/2014 Contracts and the National Authority for Research and Innovation in the frame of Nucleus Programme—contract 4N/2016.

Author details

Anita-Ioana Visan, Carmen-Georgeta Ristoscu and Ion N. Mihailescu*

*Address all correspondence to: ion.mihailescu@inflpr.ro

National Institute for Laser, Plasma and Radiation Physics, Magurele-Ilfov, Romania

References

- [1] Kalita D, Netravali AN. Interfaces in green composites: a critical review. *Reviews of Adhesion Adhesives*. 2015;3:4.
- [2] Serum Silk Fibroin [Internet]. 2016. Available from: <http://www.a6k6n6.com/Serum-Silk-Fibroin-p-8821.html> [Accessed: 2016-07-28].
- [3] Chitosan Powder [Internet]. 2016. Available from: <http://www.pureherbextract.com/chitosan-powder.html> [Accessed: 2016-07-28].
- [4] Lignin Powder [Internet]. 2016. Available from: <http://www.domtar.com/en/pulp/lignin/10387.asp> [Accessed: 2016-07-28].
- [5] Green Leaves, images free downloaded [Internet]. 2016. Available from: http://pngimg.com/upload/green_leaves_PNG3660.png [Accessed: 2016-07-28].

- [6] Sahari J, Sapuan SM. Natural fibre reinforced biodegradable polymer composites. *Reviews on Advanced Materials Science*. 2011;30:166–174.
- [7] Mohanty AK, Misra M, Drzal LT. (ed.). *Natural Fibers, Biopolymers, and Biocomposites*. Taylor & Francis Group; ISBN 9780849317415, United Kingdom, 2005.
- [8] Ha TL, Quan TM, Vu DN, Si DM. Naturally Derived Biomaterials: Preparation and Application. In: *Andrades JA. (ed.). Chapter 11 in Regenerative Medicine and Tissue Engineering*. InTech; Croatia; 2013. p. 247–274. ISBN 978-953-51-1108-5. <http://dx.doi.org/10.5772/55668>
- [9] Raquez J-M, Deléglise M, Lacrampe M-F, Krawczak P. Thermosetting (bio) materials derived from renewable resources: a critical review. *Progress in Polymer Science*. 2010;35:487–509.
- [10] Gandini A. Polymers from renewable resources: a challenge for the future of macromolecular materials. *Macromolecules*. 2008;41(24):9491–9504.
- [11] Belgacem MN, Gandini A. (ed.). *Monomers, Polymers and Composites from Renewable Resources*. Elsevier; Netherlands; 2008. ISBN:978-0-08-045316-3.
- [12] Mohanty AK, Misra M, Drzal LT. Sustainable bio-composites from renewable resources: opportunities and challenges in the green materials world. *Journal of Polymers and the Environment*. 2002;10(1):19–26.
- [13] Uyama H, Kuwabara M, Tsujimoto T, Nakano M, Usuki A, Kobayashi S. Green nanocomposites from renewable resources: plant oil–clay hybrid materials. *Chemistry of Materials*. 2003;15(13):2492–2494.
- [14] Koschuh W, Povoden G, Thang VH, Kromus S, Kulbe KD, Novalin S, Krottscheck C. Production of leaf protein concentrate from ryegrass (*Lolium perenne* × *multiflorum*) and alfalfa (*Medicago sativa* subsp. *sativa*). Comparison between heat coagulation/centrifugation and ultrafiltration. *Desalination*. 2004;163(1–3):253–259.
- [15] Yanamala N, Farcas MT, Hatfield MK, Kisin ER, Kagan VE, Geraci CL, Shvedova AA. *In Vivo* evaluation of the pulmonary toxicity of cellulose nanocrystals: a renewable and sustainable nanomaterial of the future. *ACS Sustainable Chemistry and Engineering*. 2014;2(7):1691–1698. doi:10.1021/sc500153k
- [16] Kurnia JC, Jangam SV, Akhtar S, Sasmito AP, Mujumdar AS. Advances in biofuel production from oil palm and palm oil processing wastes: a review. *Biofuel Research Journal*. 2016;3(1):332–346.
- [17] Zhang LM, You TT, Zhou T, Zhang L, Xu F. Determining Lignin degradation in white-rot fungi-treated sacrau poplar: lignin structural changes and degradation compound analysis. *Bioresources*. 2016;11(2):3972–3986.
- [18] Noreen A, Zia KM, Zuber M, Ali M, Mujahid M. A critical review of algal biomass: a versatile platform of bio-based polyesters from renewable resources. *International*

- Journal of Biological Macromolecules. 2016;86:937–949. doi:10.1016/j.ijbiomac.2016.01.067
- [19] Gandini A, Lacerda TM. From monomers to polymers from renewable resources: recent advances. *Progress in Polymer Science*. 2015;48:1–39. doi:10.1016/j.progpolymsci.2014.11.002
- [20] Luckachan GE, Mittal V. Anti-corrosion behavior of layer by layer coatings of cross-linked chitosan and poly(vinyl butyral) on carbon steel. *Cellulose*. 2015;22(5):3275–3290. doi:10.1007/s10570-015-0711-2
- [21] Zia KM, Zia F, Zuber M, Rehman S, Ahmad MN. Alginate based polyurethanes: a review of recent advances and perspective. *International Journal of Biological Macromolecules*. 2015;79:377–387. doi:10.1016/j.ijbiomac.2015.04.076
- [22] Logith Kumar R, Keshavnarayan A, Dhivya S, Chawla A, Saravanan S, Selvamurugan N. A review of chitosan and its derivatives in bone tissue engineering. *Carbohydrate Polymers*. 2016;151:172–188. doi:10.1016/j.carbpol.2016.05.049
- [23] Costa-Pinto AR, Reis RL, Neves NM. Scaffolds based bone tissue engineering: the role of chitosan. *Tissue Engineering Part B: Reviews*. 2011;17(5):331–347.
- [24] Saravanan S, Sameera DK, Moorthi A, Selvamurugan N. Chitosan scaffolds containing chicken feather keratin nanoparticles for bone tissue engineering. *International Journal of Biological Macromolecules*. 2013;62:481–486.
- [25] Jiang T, James R, Kumbar SG, Laurencin CT. Chitosan as a biomaterial: structure, properties, and applications in tissue engineering and drug delivery. *Natural and Synthetic Biomedical Polymers*. 2014;5:91–113.
- [26] Niranjana R, Koushik C, Saravanan S, Moorthi A, Vairamani M, Selvamurugan N. A novel injectable temperature-sensitive zinc doped chitosan/ β -glycerophosphate hydrogel for bone tissue engineering. *International Journal of Biological Macromolecules*. 2013;54:24–29.
- [27] Zhang BG, Myers DE, Wallace GG, Brandt M, Choong PF. Bioactive coatings for orthopaedic implants—recent trends in development of implant coatings. *International Journal of Molecular Sciences*. 2014;15(7):11878–11921.
- [28] Venkatesan J, Bhatnagar I, Manivasagan P, Kang KH, Kim SK. Alginate composites for bone tissue engineering: a review. *International Journal of Biological Macromolecules*. 2015;72:269–281.
- [29] Ma K, Cai X, Zhou Y, Zhang Z, Jiang T, Wang Y. Osteogenetic property of a biodegradable three-dimensional macroporous hydrogel coating on titanium implants fabricated via EPD. *Biomedical Materials*. 2014;9(1):015008.
- [30] Schorr D, Diouf PN, Stevanovic T. Evaluation of industrial lignins for biocomposites production. *Industrial Crops and Products*. 2014;52:65–73.

- [31] Cazacu G, Capraru M, Popa VI. Advances Concerning Lignin Utilization in New Materials. In: Thomas S, Visak PM, Mathew AP. (eds). *Advances in Natural Polymers: Composites and Nanocomposites*. New York, Heidelberg: Springer; 2013. p. 255–312.
- [32] Pan X, Gilkes N, Kadla J, Pye K, Saka S, Gregg D, Ehara K, Xie D, Lam D, Saddler J. Bioconversion of hybrid poplar to ethanol and co-products using an organosolv fractionation process: optimization of process yields. *Biotechnology and Bioengineering*. 2006;94(5):851–861.
- [33] Catignani GL, Carter ME. Antioxidant properties of lignin. *Journal of Food Science*. 1982;47:1745–1748.
- [34] Nada AMA, El-Diwanya AI, Elshafei AM. Infrared and antimicrobial studies on different lignins. *Acta Biotechnologica*. 1989;9(3):295–298.
- [35] Eraković S, Janković A, Veljović DJ, Palcevskis E, Mitrić M, Stevanović T, Janačković DJ, Mišković-Stanković V. Corrosion stability and bioactivity in simulated body fluid of silver/hydroxyapatite and silver/hydroxyapatite/lignin coatings on titanium obtained by electrophoretic deposition. *The Journal of Physics Chemistry B*. 2013;117:1633–43. doi:10.1021/jp305252a
- [36] Eraković S, Veljović DJ, Diouf PN, Stevanović T, Mitrić M, Janačković DJ, Matic IZ, Juranic ZD, Mišković-Stanković V. Investigation of silver impact on hydroxyapatite/lignin coatings electrodeposited on titanium. *Progress in Organic Coatings*. 2012;75:275–83. doi:10.1016/j.porgcoat.2012.07.005
- [37] Santillán MJ, Quaranta NE, Boccaccini AR. Titania and titania–silver nanocomposite coatings grown by electrophoretic deposition from aqueous suspensions. *Surface and Coating Technology*. 2010;205:2562–71. doi:10.1016/j.surfcoat.2010.10.001
- [38] Pique A. Deposition of Polymers and Biomaterials Using the Matrix-Assisted Pulsed Evaporation (MAPLE) Process. In: Eason R. (ed.). *Pulsed Laser Deposition of Thin Films. Applications-Led Growth of Functional Materials*. Hoboken, NJ: Wiley Interscience; 2007. p. 63–84.
- [39] Mihailescu IN, Ristoscu C, Bigi A, Mayer I. Advanced Biomimetic Implants Based on Nanostructured Coatings Synthesized by Pulsed Laser Technologies. In: Miotello A, Ossi PM. (eds.). *Laser-Surface Interactions for New Materials Production Tailoring Structure and Properties*, Series: Springer Series in Materials Science; Springer; New York City; USA; 2010. p. 235–260.
- [40] Lawrence CJ. The mechanics of spin coating of polymer-films. *Physics of Fluids*. 1988;31(10):2786–2795. doi:10.1063/1.866986
- [41] Brinker CJ, Frye GC, Hurd AJ, Ashley CS. Fundamentals of sol-gel dip coating. *Thin Solid Films*. 1991;201:97–108.

- [42] Berger LM. Coatings by Thermal Spray. *Comprehensive Hard Materials*, vol. 1. 2014. p. 471–506. 1st Edition from Vinod Sarin. ISBN-9780080965277, Elsevier; Netherlands; 2014.
- [43] Duocastella M, Fernández-Pradas JM, Morenza J, Serra P. Printing biological solutions through laser induced forward transfer. *Applied Physics A*. 2008;93:941.
- [44] Mihailescu IN, Bigi A, Gyorgy E, Ristoscu C, Sima F, Toksoy Oner E. Biomaterial Thin Films by Soft Pulsed Laser Technologies for Biomedical Applications. In: Ossi PM, Castillejo M, Zhigilei L. (eds.). *Lasers in Materials Science: Springer Series Materials in Science*. Springer; London; 2014. p. 271–291.
- [45] Sima F, Axente E, Iordache I, Luculescu C, Gallet O, Anselme K, Mihailescu IN. Combinatorial matrix assisted pulsed laser evaporation of a biodegradable polymer and fibronectin for protein immobilization and controlled release. *Applied Surface Science*. 2014;306:75–79.
- [46] McCormick RD, Lenhardt J, Stiff-Roberts AD. Effects of emulsion-based resonant infrared matrix assisted pulsed laser evaporation on the molecular weight of polymers. *Polymers*. 2012;4(1):341–354.
- [47] Gittard SD, Narayan R. Laser direct writing of micro- and nano-scale medical devices. *Expert Review of Medical Devices*. 2010;7(3):343–356.
- [48] Volpati D, Machado AD, Olivati CA, Alves N, Curvelo AAS, Pasquini D, Constantino CJL. Physical vapor deposited thin films of Lignins extracted from sugar cane bagasse: morphology, electrical properties, and sensing applications. *Biomacromolecules*. 2011;12(9):3223–3231. doi:10.1021/bm200704m
- [49] Eraković S, Janković A, Matic IZ, Juranić ZD, Vukašinović-Sekulić M, Stevanović T, Mišković-Stanković V. Investigation of silver impact on hydroxyapatite/lignin coatings electrodeposited on titanium. *Materials Chemistry and Physics*. 2013;142(2–3): 521–53.
- [50] Xin-Xing F, Li-Li Z, Jian-Yong C, Hua-Peng Z. Preparation, characterization, and properties of nano-TiO₂/silk fibroin hybrid films by sol-gel processing. *Journal of Biomedical Materials Research Part A*. 2008;84A(3):761–768.
- [51] Hoeger IC, Filpponen I, Martin-Sampedro R, Johansson LS, Österberg M, Laine J, Kelley S, Rojas OJ. Bicomponent lignocellulose thin films to study the role of surface lignin in cellulolytic reactions. *Biomacromolecules*. 2012;13(10):3228–3240. doi:10.1021/bm301001q
- [52] Aadil KR, Barapatre A, Jha H. Synthesis and characterization of Acacia lignin-gelatin film for its possible application in food packaging. *Bioresources and Bioprocessing*. 2016;3(27). doi:10.1186/s40643-016-0103-y; in press <http://link.springer.com/article/10.1186/s40643-016-0103-y> (last access September 6, 2016).

- [53] Janković A, Eraković S, Ristoscu C, Mihailescu Serban N, Duta L, Visan A, Stan GE, Popa AC, Husanu MA, Luculescu CR, Srdić VV, Janačković DJ, Mišković-Stanković V, Bleotu C, Chifiriuc MC, Mihailescu IN. Structural and biological evaluation of lignin addition to simple and silver-doped hydroxyapatite thin films synthesized by matrix-assisted pulsed laser evaporation. *Journal of Materials Science: Materials in Medicine*. 2015;26(1):5333. doi:10.1007/s10856-014-5333-y
- [54] Visan A, Stan GE, Ristoscu C, Popescu-Pelin G, Sopronyi M, Besleaga C, Luculescu C, Chifiriuc MC, Hussien MD, Marsan O, Kergourlay E, Grossin D, Brouillet F, Mihailescu IN. Combinatorial MAPLE deposition of antimicrobial orthopedic maps fabricated from chitosan and biomimetic apatite powders. *International Journal of Pharmaceutics*. 2016;511(1):505–515. doi:10.1016/j.ijpharm.2016.07.015
- [55] Axente E, Sima F, Ristoscu C, Mihailescu N, Mihailescu IN. Biopolymer Thin Films Synthesized by Advanced Pulsed Laser Techniques. In: Parveen F.K. (ed.). Chapter 4 in book *Recent Advances in Biopolymers*. ISBN 978-953-51-2255-5. InTech; Croatia; 2016.
- [56] Chrisey D, Pique A, McGill R, Horwitz J, Ringeisen B, Bubb D. Laser deposition of polymer and biomaterial films. *Chemical Reviews*. 2003;103(2):553–76.
- [57] Cristescu R, Mihailescu IN, Jelinek M, Chrisey D. Functionalized Thin Films and Structures Obtained by Novel Laser Processing Issues. *Functional Properties of Nanostructured Materials*. Springer; New York City; USA; 2006. p. 211–26.
- [58] Meredith JC, Karim A, Amis EJ. High-throughput measurement of polymer blend phase behavior. *Macromolecules*. 2000;33:5760–5762.
- [59] Li X, Nan K, Shi S, Chen H. Preparation and characterization of nano-hydroxyapatite/chitosan cross-linking composite membrane intended for tissue engineering. *International Journal of Biological Macromolecules*. 2012;50:43–49.
- [60] Torricelli P, Sima F, Axente E, Fini M, Mihailescu IN, Bigi A. Strontium and zoledronate hydroxyapatites graded composite coatings for bone prostheses. *Journal of Colloid Interface Science*. 2015;448:1–7.
- [61] Axente E, Sima F, Sima LE, Erginer M, Eroglu MS, Serban N, Ristoscu C, Petrescu SM, Oner ET, Mihailescu IN. Combinatorial MAPLE gradient thin film assemblies signaling to human osteoblasts. *Biofabrication*. 2014;6:035010.
- [62] Sima F, Axente E, Sima LE, Tuyel U, Eroglu MS, Serban N, Ristoscu C, Petrescu SM, Oner ET, Mihailescu IN. Combinatorial matrix-assisted pulsed laser evaporation: single-step synthesis of biopolymer compositional gradient thin film assemblies. *Applied Physics Letters*. 2012;101:233705.
- [63] Miroiu FM, Socol G, Visan A, Stefan N, Craciun D, Craciun V, Dorcioman, Mihailescu IN, Sima LE, Petrescu SM, Andronie A, Stamatina I, Moga S, Ducu C. Composite biocompatible hydroxyapatite–silk fibroin coatings for medical implants obtained by

- matrix assisted pulsed laser evaporation. *Materials Science and Engineering B*. 2010;169:151–158.
- [64] Miroiu FM, Stefan N, Visan A, Nita C, Luculescu C, Rasoga O, Socol M, Zgura I, Cristescu R, Craciun D, Socol G. Composite biodegradable biopolymer coatings of silk fibroin – poly(3-hydroxybutyric-acid-co-3-hydroxyvaleric-acid) for biomedical applications. *Applied Surface Science*. 2015;355:1123–1131.
- [65] Socol G, Preda N, Socol M, Sima L, Luculescu CR, Sima F, Miroiu M, Axente E, Visan A, Stefan N, Cristescu R, Dorcioman G, Stanculescu A, Radulescu L, Mihailescu IN. MAPLE deposition of PLGA micro-and nanoparticles embedded into polymeric coatings. *Digest Journal of Nanomaterials and Biostructures*. 2013;8(2):621–630.
- [66] Cristescu R, Visan A, Socol G, Surdu AV, Oprea AE, Grumezescu AM, Chifiriuc MC, Boehm RD, Yamaleyeva D, Taylor M, Narayan RJ, Chrisey DB. Antimicrobial activity of biopolymeric thin films containing flavonoid natural compounds and silver nanoparticles fabricated by MAPLE: a comparative study. *Applied Surface Science*. 2015;336:234–239. doi:10.1016/j.apsusc.2015.11.252
- [67] Erakovic S, Jankovic A, Tsui GCP, Tang C-Y, Miskovic-Stankovic V, Stevanovic T. Novel bioactive antimicrobial Lignin containing coatings on titanium obtained by electrophoretic deposition. *International Journal of Molecular Sciences*. 2014;15(7):12294–12322. doi:10.3390/ijms150712294
- [68] Erakovic S, Veljovic D, Diouf PN, Stevanovic T, Mitric M, Milonjic S, Miskovic-Stankovic VB. Electrophoretic deposition of biocomposite Lignin/hydroxyapatite coatings on titanium. *International Journal of Chemical Reactor Engineering*. 2009;7:A62.
- [69] Yoshida A, Miyazaki T, Ishida E, Ashizuka M. Preparation of bioactive chitosan-hydroxyapatite nanocomposites for bone repair through mechanochemical reaction. *Materials Transactions*. 2004;45:994–998.
- [70] Ito M, Hidaka Y, Nakajima M, Yagasaki H, Kafrawy AH. Effect of hydroxyapatite content on a physical properties and connective tissue reactions to a chitosan-hydroxyapatite composite membrane. *Journal of Biomedical Materials Research*. 1999;45:204–208.
- [71] Zhang Y, Zhang M. Calcium/phosphate composite scaffolds for controlled *in vitro* antibiotic drug release. *Journal of Biomedical Materials Research*. 2002;62:378–386.
- [72] Sivakumar M, Manjubala I, Panduranga Rao K. Preparation, characterization and *in vitro* release of gentamicin from coralline hydroxyapatite-chitosan composite microspheres. *Carbohydrate Polymers*. 2002;49:281–288.
- [73] Hu Q, Li B, Wang M, Shen J. Preparation and characterization of biodegradable chitosan/hydroxyapatite nanocomposite rods via *in situ* hybridization: a potential material as internal fixation of bone fracture. *Biomaterials*. 2004;25:779–785.

- [74] Davidenko N, Carrodegua RG, Peniche C, Solís Y, Cameron RE. Chitosan/apatite composite beads prepared by *in situ* generation of apatite or Si-apatite nanocrystals. *Acta Biomaterialia*. 2010;6:466–476.
- [75] Thein-Han WW, Misra RDK. Biomimetic chitosan–nanohydroxyapatite composite scaffolds for bone tissue engineering. *Acta Biomaterialia*. 2009;5:1182–1197.
- [76] Boyan BD, Lincks J, Lohmann CH, Sylvia VL, Cochran DL, Blanchard CR, Dean DD, Schwartz Z. Effect of surface roughness and composition on costochondral chondrocytes is dependent on cell maturation state. *Journal of Orthopaedic Research*. 1999;17:446–457.